Electronic Supplementary Material (ESI) for Inorganic Chemistry Frontiers.
This journal is © the Partner Organisations 2016

Supporting Information for

Two-step warming solvothermal syntheses, luminescence and slow magnetic relaxation of isostructural dense LnMOFs based on nanoscale 3-connected linkers

Cai-Ming Liu,[a,*] De-Qing Zhang,[a] Yong-Sheng Zhao,[b] Xiang Hao,[a] and Dao-Ben Zhu[a]

[a]*Beijing National Laboratory for Molecular Sciences, Center for Molecular Science, Key Laboratory of Organic Solids，Institute of Chemistry, Chinese Academy of Sciences, Beijing 100190, P.R. China*
[b]*Key Laboratory of Photochemistry, Institute of Chemistry, Chinese Academy of Sciences, Beijing 100190, P. R. China*

Table S1. Continuous Shape Measures calculation for the Dy(III) ion in **2**.

```
-------------------------------------------------------------------------------
S H A P E   v2.1         Continuous Shape Measures calculation
(c) 2013  Electronic Structure Group, Universitat de Barcelona
                    Contact:  llunell@ub.edu
-------------------------------------------------------------------------------

Dy structures

OP-8            1 D8h   Octagon
HPY-8           2 C7v   Heptagonal pyramid
HBPY-8          3 D6h   Hexagonal bipyramid
CU-8            4 Oh    Cube
SAPR-8          5 D4d   Square antiprism
TDD-8           6 D2d   Triangular dodecahedron
JGBF-8          7 D2d   Johnson gyrobifastigium J26
JETBPY-8        8 D3h   Johnson elongated triangular bipyramid J14
JBTPR-8         9 C2v   Biaugmented trigonal prism J50
BTPR-8         10 C2v   Biaugmented trigonal prism
```

JSD-8	11	D2d	Snub diphenoid J84
TT-8	12	Td	Triakis tetrahedron
ETBPY-8	13	D3h	Elongated trigonal bipyramid

Structure [ML8]	OP-8	HPY-8	HBPY-8	CU-8	SAPR-8	TDD-8	JGBF-8	JETBPY-8	JBTPR-8	BTPR-8	JSD-8	TT-8	ETBPY-8
ABOXIY	, 31.941,	22.824,	15.754,	11.389,	2.217,	2.236,	13.936,	26.951,	1.529,	1.657,	3.526,	11.450,	23.937

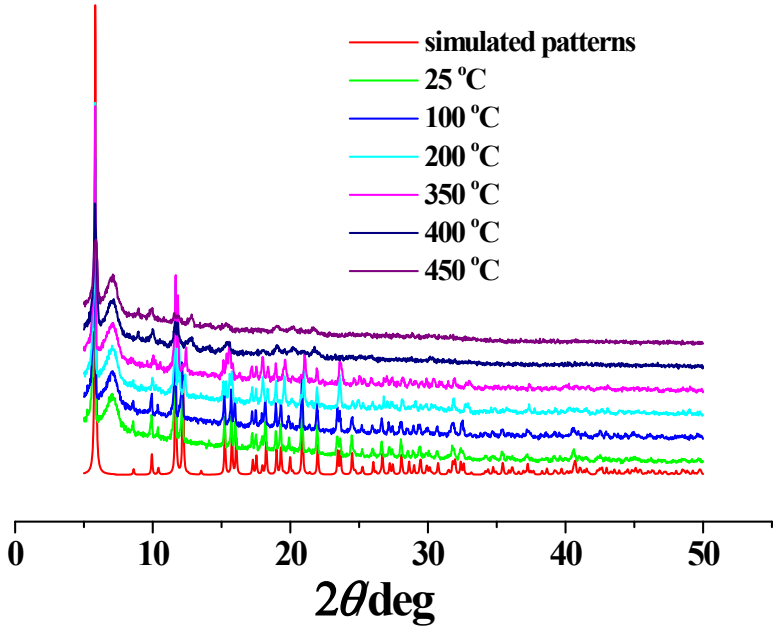

Fig. S1. The simulative X-ray diffraction pattern and X-ray thermodiffractogram of **1** under air from 25 to 450 °C (the broad peak at around 7° of 2θ diffraction angle comes from the background of Al_2O_3).

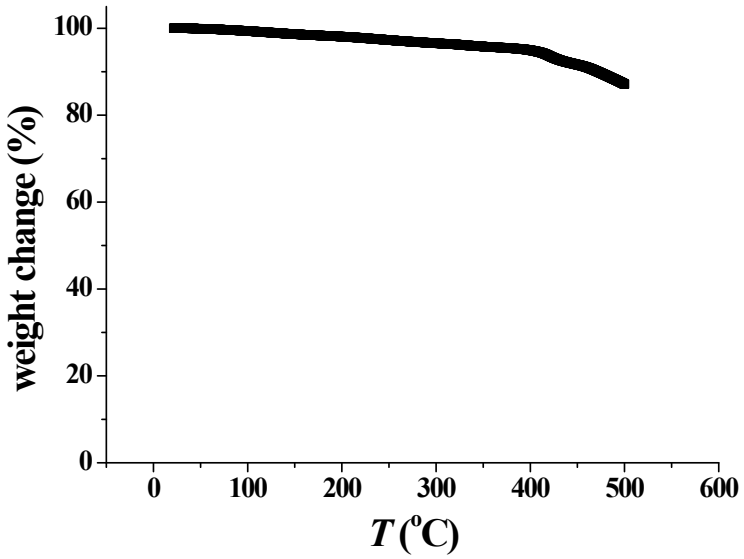

Fig. S2. TGA curve for complex **1**.

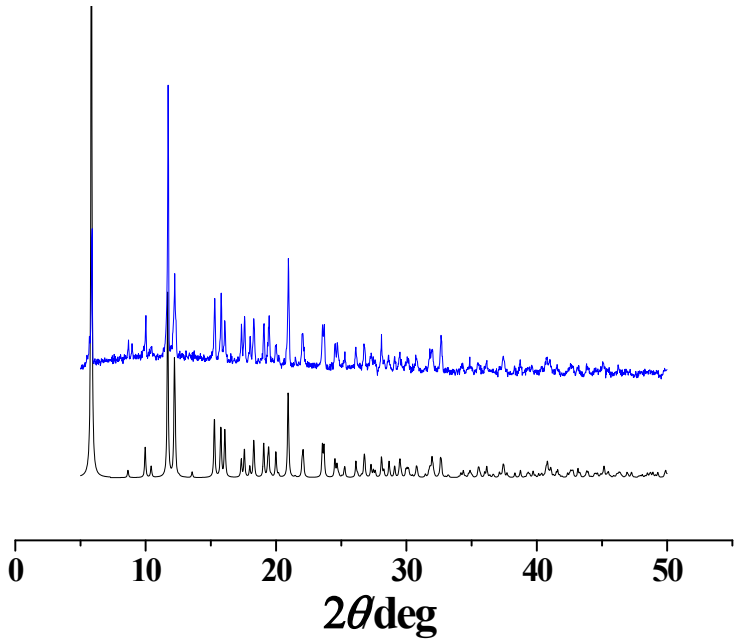

Fig. S3. The simulative (black) and experimental (blue, at room temperature) powder X-ray diffraction patterns for **2**.

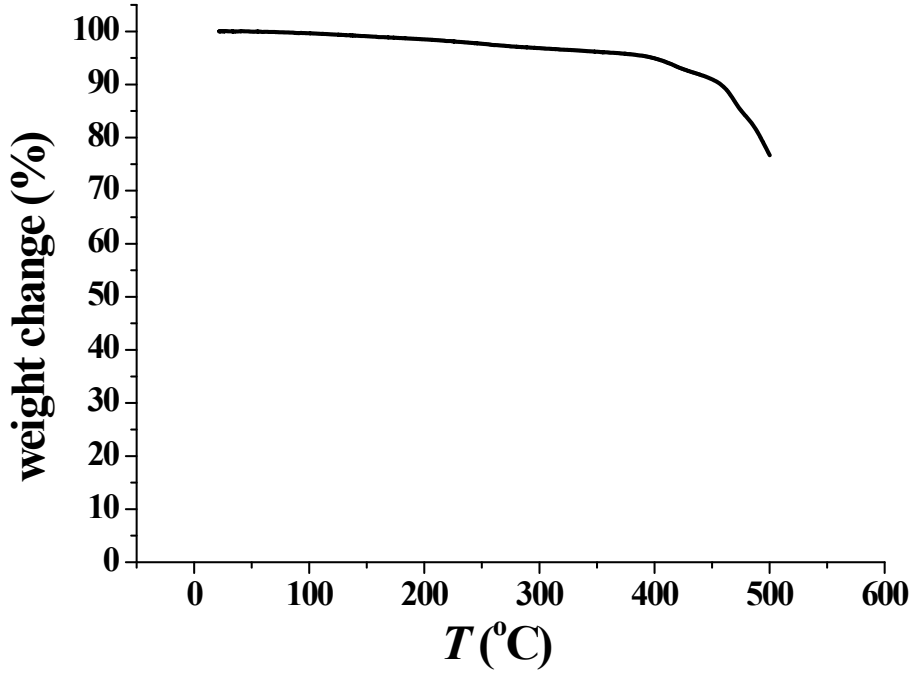

Fig. S4. TGA curve for complex **2**.

Table S2. Potential void volume of LnMOFs based on the BTB^{3-} ligand.

Compounds	Potential void volume	Reference
$Tb(BTB)(H_2O)\cdot 2(C_6H_{12}O)$	$S_{Langmuir}$ = 1330 m^2g^{-1}	7a
$Ce(BTB)(H_2O)$	$S_{Connolly}$ = 1797 m^2g^{-1}	7b
$La(BTB)(H_2O)\cdot 3DMF$	$S_{Langmuir}$ = 1385 m^2g^{-1}; 51.9% (by PLATON)	7c
$[Gd(BTB)(DMSO)_2]\cdot H_2O$	49.8% (by PLATON)	7d
$[Eu_{1.5}(BTB)_{1.5}(H_2O)]\cdot 3DMF$	38.5% (by PLATON)	7e
$[Ln(BTB)H_2O]$	7.7% (by PLATON)	This work

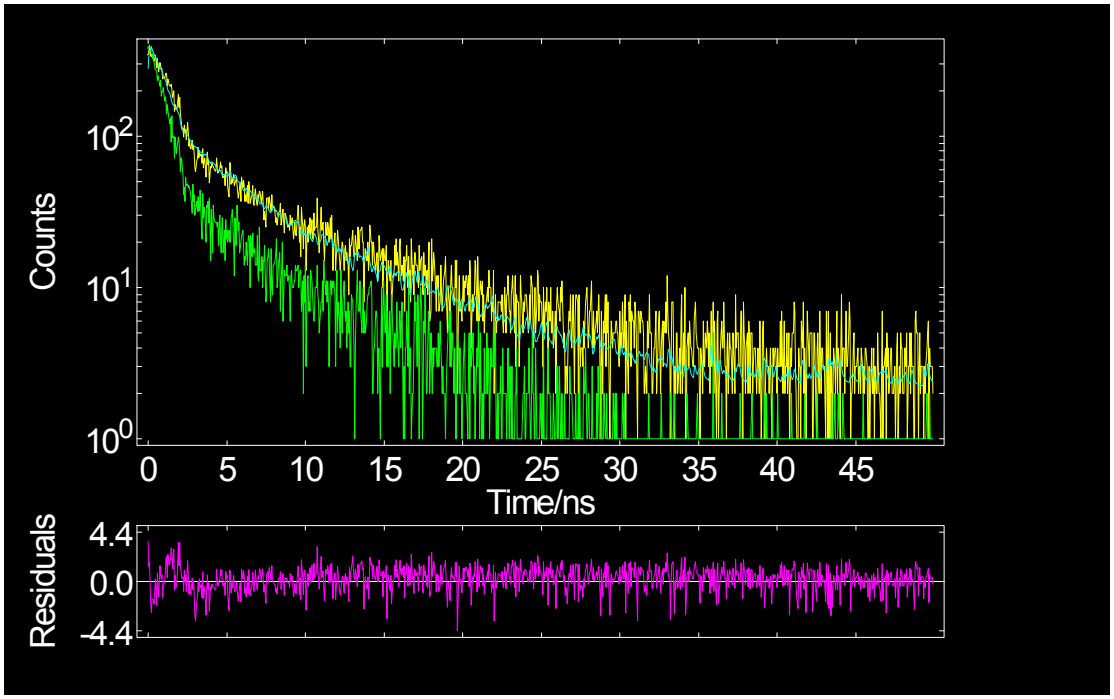

Fit Parameters

Fit = $A + B_1.\exp(-t/\tau_1) + B_2.\exp(-t/\tau_2)$

	Value	Std Dev		Value	Std Dev	Rel %
τ_1	2.468E-9	1.191E-10	B_1	1.141E-2	7.932E-4	34.50
τ_2	1.125E-10	7.229E-12	B_2	4.754E-1	2.658E-2	65.50
A	2.134E+0					

Fig. S5. $^5D_0$ decay for fluorescence and fitted curves of complex **1** measured at room temperature. Emission was monitored at 612 nm and the excitation was performed at 395 nm.

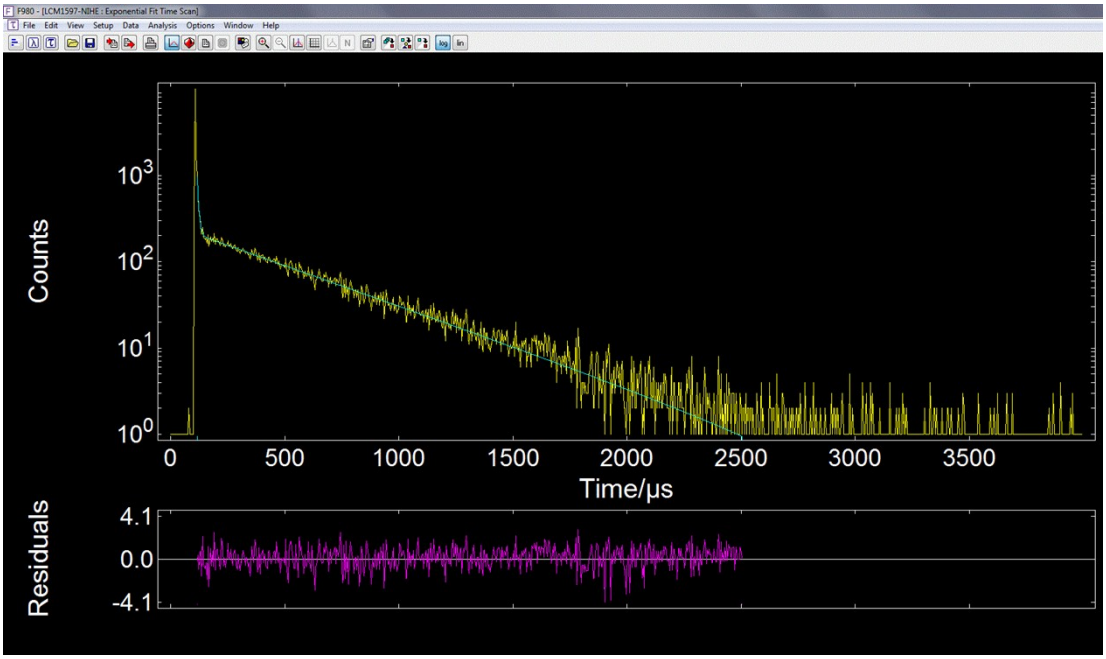

Fit Parameters

Fit = $A + B_1.\exp(-t/\tau_1) + B_2.\exp(-t/\tau_2)$

	Value	Std Dev		Value	Std Dev	Rel %
τ_1	6.40	0.33	B_1	1399.25	341.49	8.49
τ_2	463.98	5.85	B_2	206.80	9.16	65.50
A	-0.615					

Fig. S6. $^5D_0$ decay for phosphorescence and fitted curves of complex **1** measured at room temperature. Emission was monitored at 612 nm and the excitation was performed at 395 nm.

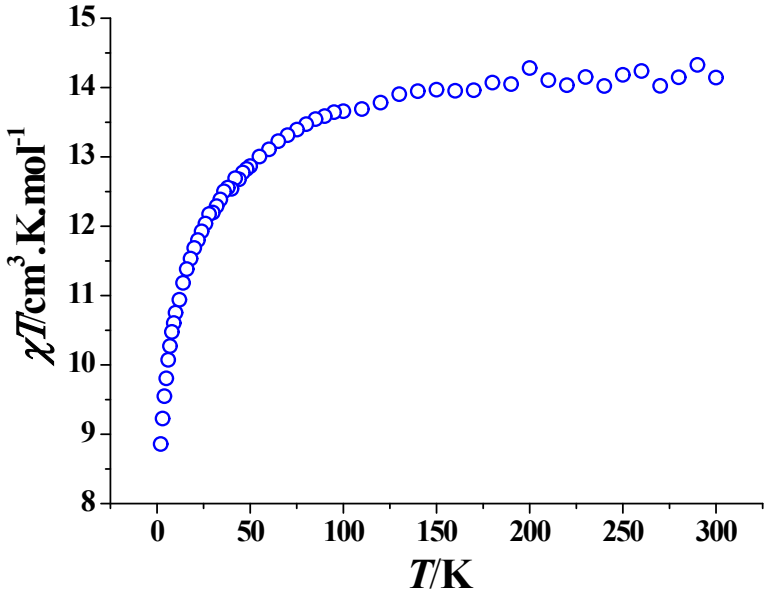

Fig. S7. χT versus T plot of **2**.

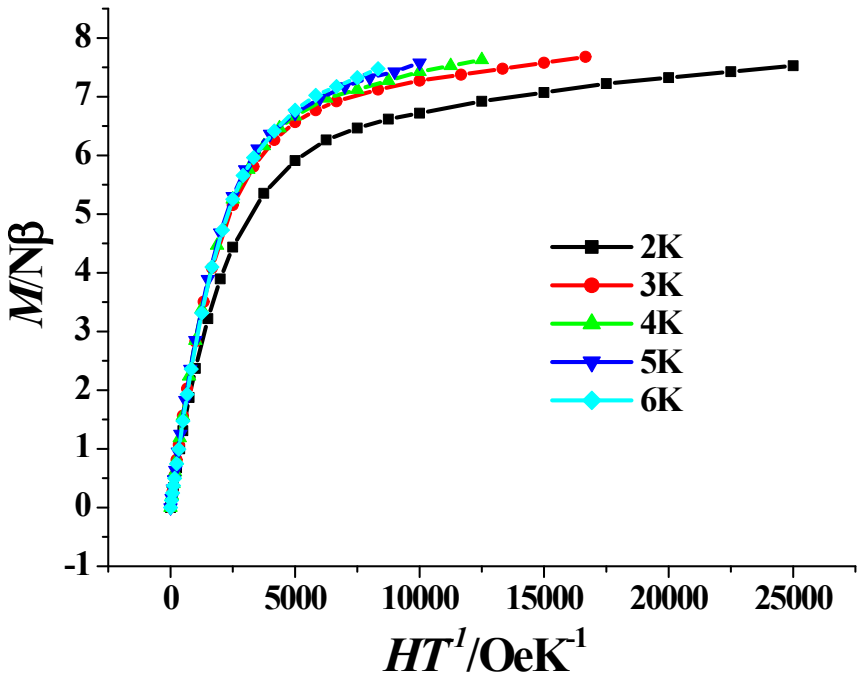

Fig. S8. M versus H/T plots at 2–6 K of **2**.

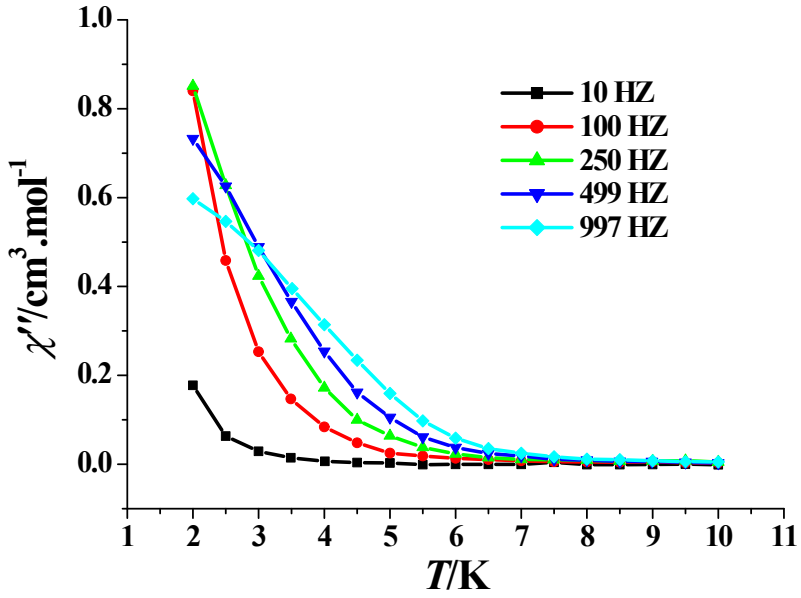

Fig. S9. χ'' versus T plots measured in a 2.5 Oe ac magnetic field with a zero dc field for **2.**

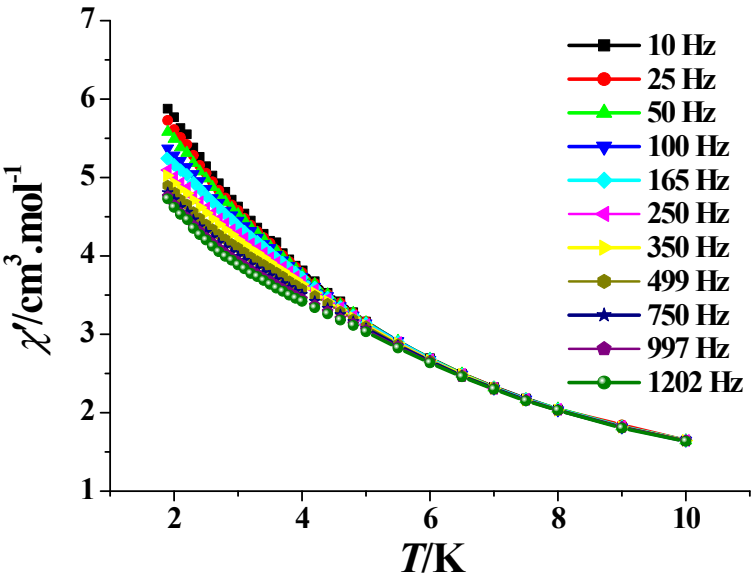

Fig. S10. χ' versus T plots measured in a 2.5 Oe ac magnetic field with a 1000 Oe dc field for **2.**

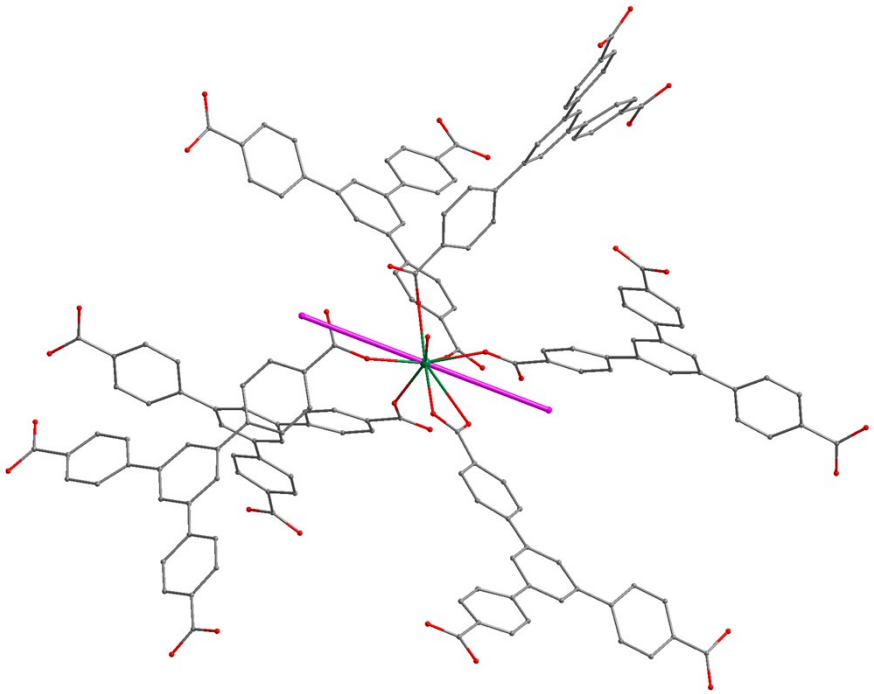

Fig. S11. Magnetic axis of the Dy^{3+} ion in **2** calculated by an electrostatic method.

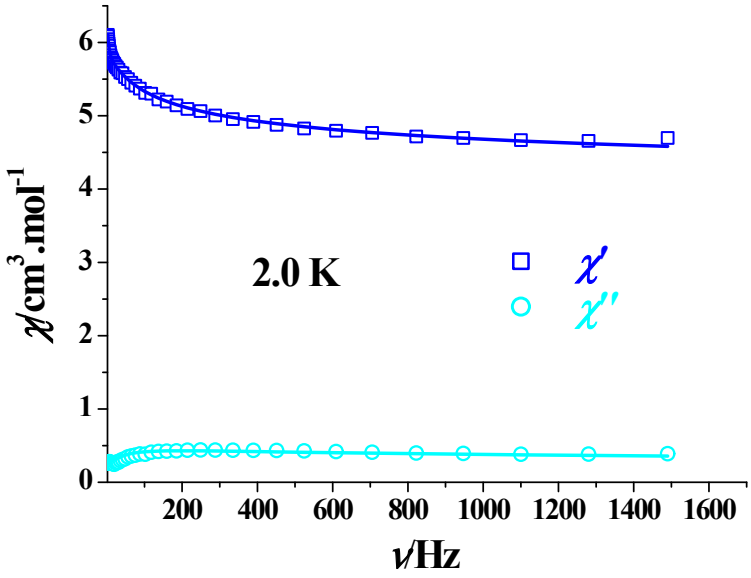

Fig. S12. Frequency dependence of the in-phase (χ', top) and out-of-phase (χ'', bottom) ac susceptibility of **2** at 2.0 K. the solid lines represent the best fitting with the sum of two modified Debye functions.

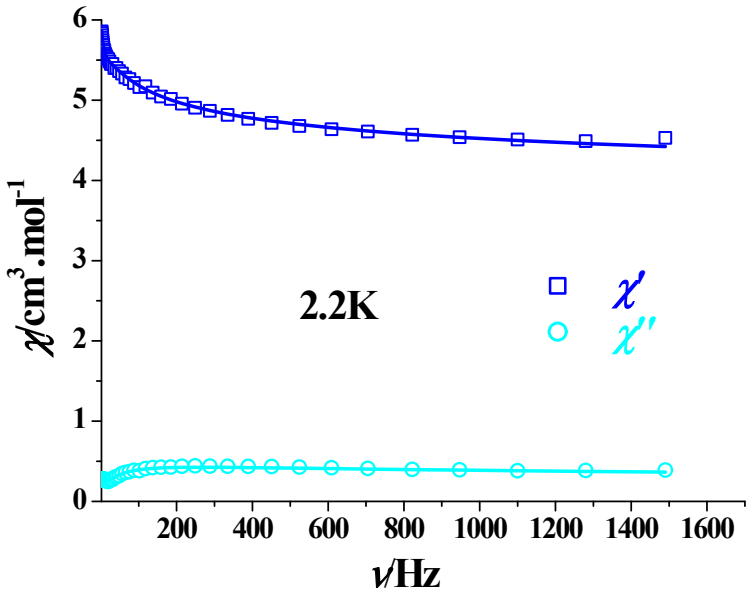

Fig. S13. Frequency dependence of the in-phase (χ', top) and out-of-phase (χ'', bottom) ac susceptibility of **2** at 2.2 K. the solid lines represent the best fitting with the sum of two modified Debye functions.

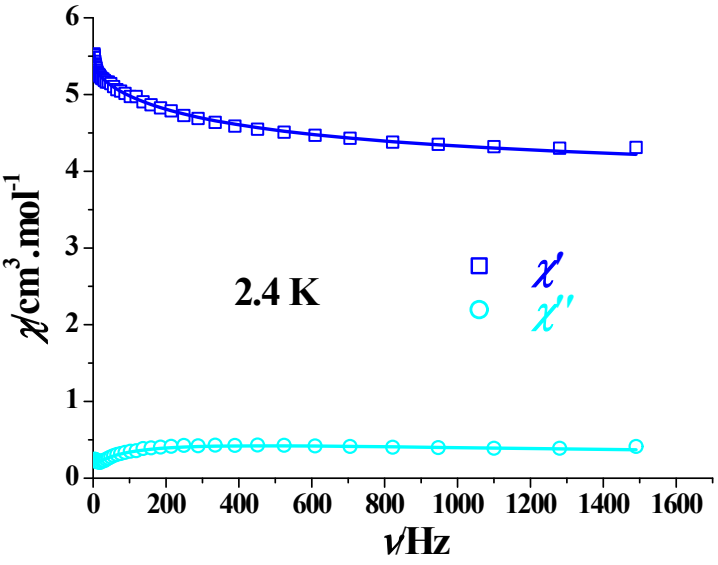

Fig. S14. Frequency dependence of the in-phase (χ', top) and out-of-phase (χ'', bottom) ac susceptibility of **2** at 2.4 K. the solid lines represent the best fitting with the sum of two modified Debye functions.

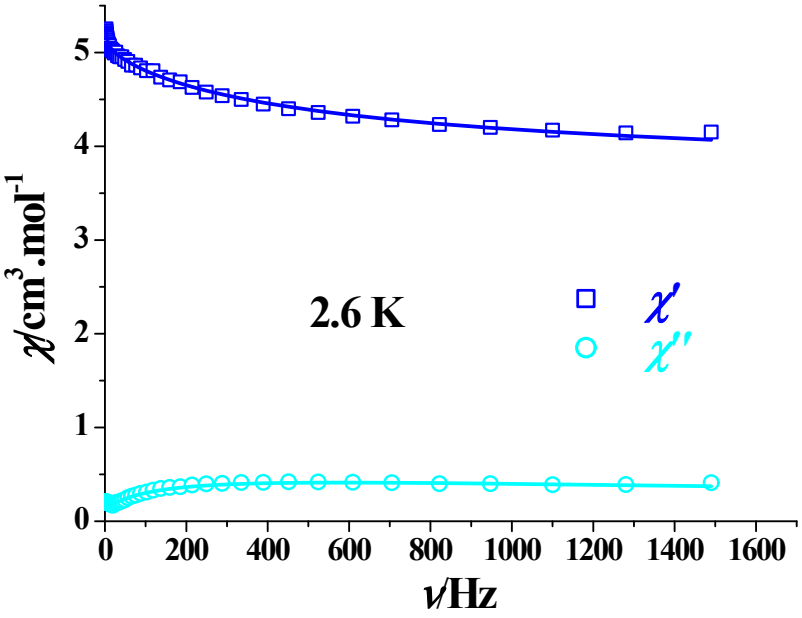

Fig. S15. Frequency dependence of the in-phase (χ', top) and out-of-phase (χ'', bottom) ac susceptibility of **2** at 2.6 K. the solid lines represent the best fitting with the sum of two modified Debye functions.

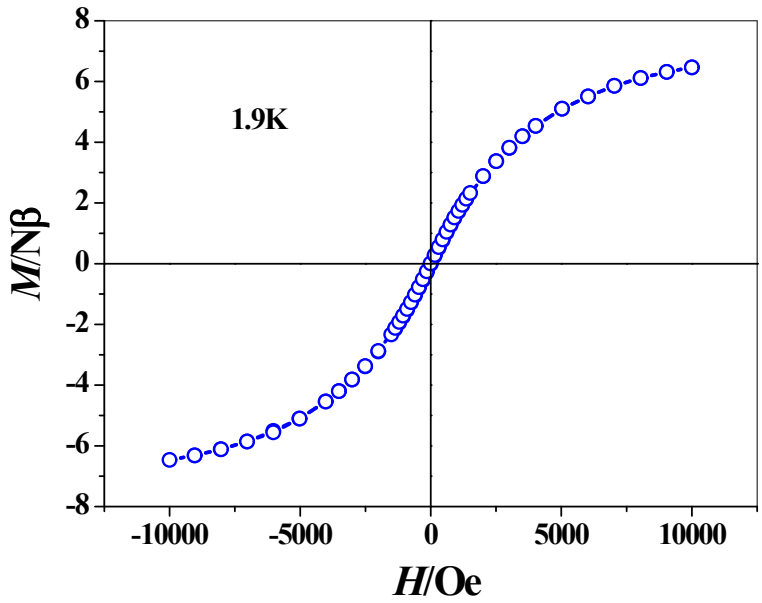

Fig. S16. Plot of *M* versus *H* at 1.9 K from −10000 to 10000 Oe for **2**.

Table S3. Linear combination of two modified Debye model fitting parameters at 2.0-2.6 K of **2** under 1 kOe dc field.

T(K)	χ_2(cm^3.mol^{-1})	χ_1(cm^3.mol^{-1})	χ_0(cm^3.mol^{-1})	τ_1(s)	α_1	τ_2(s)	α_2
2.0	6.8539	3.44511	3.71894	0.008	1.863E-7	0.00204	0.65798
2.2	6.46216	3.24677	3.56324	0.00669	0.00019	0.00145	0.64117
2.4	5.75198	4.02202	3.68468	0.05961	0.00006	0.00033	0.42496
2.6	5.49167	3.89797	3.54221	0.06924	0.03696	0.00027	0.39353

The sum of two modified Debye functions:

$$\chi_{ac}(\omega) = \frac{\chi_2 - \chi_1}{1 + (i\omega\tau_2)^{(1-\alpha_2)}} + \frac{\chi_1 - \chi_0}{1 + (i\omega\tau_1)^{(1-\alpha_1)}} + \chi_0 \quad (1)$$

$$\chi' = \frac{(\chi_2 - \chi_1)[1 + (\omega\tau_2)^{1-\alpha_2}\sin 1/2\alpha_2\pi]}{1 + 2(\omega\tau_2)^{(1-\alpha_2)}\sin 1/2\alpha_2\pi + (\omega\tau_2)^{2(1-\alpha_2)}} + \frac{(\chi_1 - \chi_0)[1 + (\omega\tau_1)^{1-\alpha_1}\sin 1/2\alpha_1\pi]}{1 + 2(\omega\tau_1)^{(1-\alpha_1)}\sin 1/2\alpha_1\pi + (\omega\tau_1)^{2(1-\alpha_1)}} + \chi_0 \quad (2)$$

$$\chi'' = \frac{(\chi_2 - \chi_1)[(\omega\tau_2)^{1-\alpha_2}\cos 1/2\alpha_2\pi]}{1 + 2(\omega\tau_2)^{(1-\alpha_2)}\sin 1/2\alpha_2\pi + (\omega\tau_2)^{2(1-\alpha_2)}} + \frac{(\chi_1 - \chi_0)[(\omega\tau_1)^{1-\alpha_1}\cos 1/2\alpha_1\pi]}{1 + 2(\omega\tau_1)^{(1-\alpha_1)}\sin 1/2\alpha_1\pi + (\omega\tau_1)^{2(1-\alpha_1)}} + \chi_0 \quad (3)$$